Slip velocity and Knudsen layer in the lattice Boltzmann method for microscale flows

Seung Hyun Kim* and Heinz Pitsch
Department of Mechanical Engineering, Stanford University, California 94305-3035, USA

Iain D. Boyd
Department of Aerospace Engineering, University of Michigan, Michigan 48109-2140, USA

(Received 17 August 2007; revised manuscript received 18 December 2007; published 13 February 2008)

We present mesoscopic fluid-wall interaction models for lattice Boltzmann (LB) model simulations of microscale flows. The exact solution of the slip velocity for the LB equation with the Bhatnagar-Gross-Krook collision operator is obtained for Poiseuille flow at finite Knudsen numbers. With a consistent definition of the Knudsen number, the slip coefficients of the LB equation with the standard D2Q9 scheme are found to be slightly larger than those of the Boltzmann equation with the same boundary condition, which makes the standard LB method remain quantitatively accurate only for small Knudsen numbers. By modifying the nonequilibrium energy flux or introducing the effective relaxation time, the LB method is analytically shown to reproduce the slip phenomena up to second order in the Knudsen number. For the standard LB method, the Knudsen layer is captured only with modification of the relaxation dynamics such as in the effective relaxation time model.

DOI: 10.1103/PhysRevE.77.026704 PACS number(s): 47.11.−j, 47.61.−k, 05.20.Dd

I. INTRODUCTION

In the classical hydrodynamic theory, fluid motions in the bulk are described by the Navier-Stokes equations [1]. For fluid-wall interactions, it is postulated that, at the macroscopic level, fluid just outside the wall moves with the same velocity as the wall: the so-called no-slip condition [1]. This macroscopic description works well when kinetic effects present in the vicinity of the wall boundary are negligible at the macroscale. For flows in micro- and nanoscale devices [2], as the characteristic flow length scale becomes comparable to the molecular mean free path, the kinetic effects and the microscopic details of fluid-wall interactions become important even at the macroscale. The flow in this regime is characterized by the Knudsen number $\mathrm{Kn}=\lambda/H$, where λ is the mean free path of the molecules and H is the characteristic length scale of the flow [3,4]. At small Kn—e.g., $0.01<\mathrm{Kn}<0.1$—the kinetic effects first appear at the macroscopic level as the slip motion near the wall. At higher Kn, the kinetic boundary layer occupies a significant portion of the flow and the application of the Navier-Stokes equations to the whole flow field is invalid [3].

The modeling of micro- and nanoscale flows has recently been an active area of research for the lattice Boltzmann (LB) method [5–18]. The first analysis of the slip velocity in the LB method was presented in Cornubert *et al.* [19], where the appearance of the slip velocity in Couette flows was demonstrated analytically and numerically for the bounce-back and specular reflection boundary conditions [19]. The exact solution for the slip velocity in Poiseuille flow was first presented in Ginzburg and Adler [20], together with the exact population solution using the face-centered hypercubic (FCHC) multiple-relaxation-time (MRT) model [20–23]. The analytic solutions for the so-called D2Q9 scheme [7,9] were also reported for the MRT and single-relaxation-time Bhatnagar-Gross-Krook (BGK) models [6] with the bounce-back boundary condition [24,25]. The major focus in these studies [20,24,25] was, however, on accurate implementation of the no-slip boundary condition in macroscale hydrodynamics. Recent studies have revealed that the LB method produces "physical slip" flows [10–18] and that fluid-wall interaction models are of critical importance in predictions of the slip phenomena [12,18,26,27]. First attempts to predict slip phenomena in microscale flows were made by Nie *et al.* [10], Lim *et al.* [11], and Succi [28], where reflection-type boundary conditions—i.e., the bounce-back and specular reflection schemes—are proposed as a mesoscopic fluid-wall interaction model. The diffuse scattering boundary condition, which is a discrete analog of the boundary condition used in the continuum kinetic theory, has also attracted significant attention [12,15,16]. The extension to the Maxwell boundary condition with partial accommodation has also been reported [29]. In Sbragaglia and Succi [26], it was shown that a combination of the bounce-back and specular reflection boundary conditions can be designed to give the same slip velocity as that of the diffuse scattering boundary condition. Szalmas [30] presented a modified interpolation method for the slip-flow boundary located at arbitrary wall locations between the boundary lattices and the first fluid lattices. In the MRT model, the slip velocity also depends on a free kinetic relaxation parameter for higher-order nonequilibrum moments [25,31]. While encouraging results have been reported, the capability of the LB method for micro- and nanoscale flows is still being debated, in part because of different definitions of the Knudsen number in different studies [15,27,32,33].

For moderate Kn flows beyond the slip-flow regime, a higher-order LB method is needed to obtain a quantitative prediction as well as to reproduce the presence of the Knudsen layer [34,35]. In particular, Ansumali *et al.* [34] showed that in Couette flow, the Knudsen layer is captured only for

*shkcomb@stanford.edu

the higher-order LB method. While a nonperturbative analysis of the application of the standard LB method to finite Kn flows has been presented [36], it is shown in the present paper that the macroscopic equation for the standard LB method is exactly the Navier-Stokes equation for Poiseuille flows, which is consistent with the result of Ansumali *et al.* [34] for Couette flow and previous results for Poiseuille flow [24,25]. In standard lattices such as D2Q9, a modification to a relaxation dynamics such as the "wall function approach" [27] is thus essential to capture the Knudsen layer.

The objectives of this paper are to analyze the accuracy of the LB model in micro- and nanoscale flows with a consistent definition of Kn and to develop improved fluid-wall interaction models that are accurate up to second order in Kn. The LB equation with the BGK collision operator and the definition of Kn are described in Sec. II. In Sec. III, an exact solution of the slip velocity for the LB equation is obtained for Poiseuille flow at finite Kn. The effective diffuse scattering boundary condition is introduced to reproduce the first-order slip coefficient in the asymptotic solution of the Boltzmann equation. A modified LB equation is proposed to reproduce the slip phenomena to second order in Kn. The effective relaxation time model, which is the extension of the method of Zhang *et al.* [27], is analyzed with the exact solution. Discrete lattice effects in the slip velocity are discussed. The numerical simulation results are presented and compared with the direct simulation Monte Carlo (DSMC) method and the linearized Boltzmann equation solution in Sec. IV. The paper ends with a summary of the main results.

II. LATTICE BOLTZMANN METHOD

A. Discrete velocity Boltzmann equation

The discrete velocity Boltzmann (DVB)-BGK equation can be derived by projecting the Boltzmann-BGK equation onto the finite-functional space represented by the Hermite basis [37]:

$$\partial_t f_i + c_{i\alpha}\partial_\alpha f_i = -\frac{1}{\tau}(f_i - f_i^{\mathrm{eq}}) + F_i, \tag{1}$$

where f_i is the distribution function of the discrete velocity $c_{i\alpha}$, t is time, α is the spatial coordinate, τ is the relaxation time, and F_i is an external force for the velocity $c_{i\alpha}$. To recover the (isothermal) Navier-Stokes equations in the small-Kn limit, a second-order Hermite-expansion is required, and the equivalent discrete velocities and their weights are determined by the corresponding Gauss-Hermite quadrature with accuracy equal to or higher than fourth order [37]. The equilibrium distribution function and the external force term are, respectively, given by [35]

$$f_i^{\mathrm{eq}} = w_i\left[\rho + \frac{j_\alpha c_{i\alpha}}{c_s^2} + \frac{1}{2}\frac{(j_\alpha c_{i\alpha})^2}{\rho c_s^4} - \frac{1}{2}\frac{j_\alpha j_\alpha}{\rho c_s^2}\right], \tag{2}$$

$$F_i = w_i\rho\left[\frac{g_\alpha c_{i\alpha}}{c_s^2} + \frac{g_\alpha u_\beta c_{i\alpha} c_{i\beta}}{c_s^4} - \frac{g_\alpha u_\alpha}{c_s^2}\right], \tag{3}$$

where g_α is the external body force. For the D2Q9 scheme [9], the discrete velocities are given by

$$c_{i\alpha} = \begin{cases} (0,0), & \text{for } i = 0, \\ \sqrt{3}c_s(\cos[(i-1)\pi/2], \sin[(i-1)\pi/2]), & \text{for } i = 1,2,3,4, \\ \sqrt{3}c_s(\sqrt{2}\cos[(2i-9)\pi/4], \sqrt{2}\sin[(2i-9)\pi/4]), & \text{for } i = 5,6,7,8. \end{cases} \tag{4}$$

The weights are $w_0 = 4/9$, $w_1 = w_2 = w_3 = w_4 = 1/9$, and $w_5 = w_6 = w_7 = w_8 = 1/36$. The density ρ and the momentum density j_α are, respectively, given by

$$\sum_i f_i = \rho, \tag{5}$$

$$\sum_i c_{i\alpha} f_i = j_\alpha = \rho u_\alpha. \tag{6}$$

Using the Chapman-Enskog expansion, the kinematic viscosity is obtained as

$$\nu = \tau c_s^2, \tag{7}$$

where $c_s = \sqrt{RT_0}$, R is the gas constant, and T_0 is the reference temperature. The equation of state is $p = c_s^2\rho$, where p is the pressure.

B. Lattice Boltzmann equation

The LB equation can be obtained by discretizing the DVB equation for time t and space $\mathbf{x}$. By integrating Eq. (1) along the trajectory of the particle velocity $\mathbf{c}_i$ [24], we obtain

$$f_i(\mathbf{x} + \delta t\mathbf{c}_i, t + \delta t) - f_i(\mathbf{x}, t) = \int_0^{\delta t} \Omega_i(\mathbf{x} + t'\mathbf{c}_i, t + t')dt', \tag{8}$$

where $\Omega_i = -(f_i - f_i^{\mathrm{eq}})/\tau + F_i$. The integral in Eq. (8) can be approximated by

$$\int_0^{\delta t} \Omega_i(\mathbf{x} + t'\mathbf{c}_i, t + t')dt' \approx \frac{\delta t}{2}[\Omega_i(\mathbf{x} + \delta t\mathbf{c}_i, t + \delta t) + \Omega_i(\mathbf{x}, t)] + O(\delta t^2). \tag{9}$$

By introducing the transformation $\hat{f}=f-\Omega_i\delta t/2$ [38], the LB equation can be written as

$$\hat{f}_i(\mathbf{x}+\delta t\mathbf{c}_i,t+\delta t)-\hat{f}_i(\mathbf{x},t) = -\frac{\delta t}{\tau+\delta t/2}(\hat{f}_i-f_i^{\mathrm{eq}})+\frac{\tau}{\tau+\delta t/2}F_i\delta t. \quad (10)$$

The density and the momentum density are, respectively, given by

$$\rho=\sum_i \hat{f}_i, \quad (11)$$

$$j_\alpha=\sum_i c_{\alpha i}\hat{f}_i+\rho g_\alpha\frac{\delta t}{2}. \quad (12)$$

This solves the DVB equation with second order in δt. Due to the second-order accuracy, the present formulation results in correct mass and momentum conservation equations to the Navier-Stokes order, where the discrete lattice effects due to the time and spatial discretization are reduced [7,39]. With the use of the transformation $\hat{f}=f-\Omega_i\delta t/2$, the relations for the momentum and the viscosity in the DVB equation are preserved even with the time and spatial discretization in the LB equation [7,39].

For the so-called lattice units, the unit time is δt and the unit length is the distance (in a spatial coordinate) traveled by particles during δt, $\sqrt{3}c_s\delta t$. The sound speed in the lattice units is given by $c_s=1/\sqrt{3}$. It is also known that for different scalings, the sound speed can be a freely adjustable parameter [25].

C. Relaxation time and Knudsen number

In simulations of microscale flows using the LB method with the BGK collision operator, the relationship of the relaxation time τ and the mean free path λ should be provided. In the literature for the LB method, the relationship of τ and λ and the definition of Kn are diverse [10,11,13,15,27,33,40]. Since the LB-BGK equation is a discrete version of the continuous Boltzmann-BGK equation, here the mean free path for the LB method is chosen to be that for the Boltzmann-BGK equation.

The mean free path λ is an average distance traveled by a molecule before colliding with another molecule. In hard-sphere gases, it is well defined and given by [41]

$$\lambda=\frac{m}{\sqrt{2}\pi\rho d^2}, \quad (13)$$

where m and d are the mass and the diameter of the hard-sphere molecules, respectively. Using the Chapman-Enskog result of the viscosity [41],

$$\mu=\frac{5m}{16d^2}\sqrt{\frac{RT}{\pi}}, \quad (14)$$

λ can be written as

$$\lambda=\frac{\mu}{\rho}\frac{16}{5}\frac{1}{\sqrt{2\pi}}\frac{1}{\sqrt{RT}}=\frac{16}{5\pi}\sqrt{\frac{\pi}{2}}\frac{\nu}{c_s}. \quad (15)$$

The mean free path is, however, not well defined when collisions due to the intermolecular interaction are not well defined [3,42]. In that sense, the mean free path is a conceptual quantity, except for hard-sphere molecules [43]. When collisions due to the intermolecular interaction are not well defined, Cercignani [42] proposed to use the viscosity-based mean free path

$$\lambda_\nu=\frac{\mu}{p}\sqrt{\frac{\pi RT}{2}}=\sqrt{\frac{\pi}{2}}\frac{\nu}{c_s}. \quad (16)$$

The viscosity-based mean free path λ_ν is very close to the exact result for hard-sphere molecules.

The relaxation time τ in the Boltzmann-BGK equation is usually determined to match the viscosity of the bulk fluid. Using the viscosity-based mean free path, Eq. (16), the mean free path for the BGK molecules can be defined as

$$\lambda=\sqrt{\frac{\pi}{2}}\frac{\nu}{c_s}=\sqrt{\frac{\pi}{2}}\tau c_s. \quad (17)$$

The Knudsen number is thus given by

$$\mathrm{Kn}=\frac{\lambda}{H}=\sqrt{\frac{\pi}{2}}\frac{\nu}{c_sH}=\sqrt{\frac{\pi}{2}}\frac{\tau c_s}{H}. \quad (18)$$

This is the relationship of the relaxation time and the Knudsen number in the LB method adopted here. This relationship has also been proposed by arguing the consistency of the definition of Kn for hard-sphere molecules in the small-Kn limit [33].

In the description of experimental results, the viscosity-based mean free path is widely used to define Kn. However, considering the nature of the mean free path described above, the definition of the mean free path can be different for different studies, except for hard-sphere molecules [34]. The only consistency condition that should be satisfied, when comparing the solution of the LB equation with those of other reference methods, is then the equivalence of Kn in the LB method and that in the reference methods.

III. ANALYTIC SOLUTION OF THE SLIP VELOCITY

A. Linearized Boltzmann-BGK equation

The slip velocity in the kinetic theory [44] is given by

$$u_s=c_1\lambda\left.\frac{\partial u}{\partial n}\right|_w+c_2\lambda^2\left.\frac{\partial^2 u}{\partial^2 n}\right|_w, \quad (19)$$

where n is the wall normal coordinate pointing into the fluid and the subscript w denotes the quantity at the wall. For full accommodation conditions, where all reflected particles are equilibrated with a wall, the slip coefficients are given by $c_1=1.1466$ and $c_2=-0.975\,66$ [44,45]. These values of the slip coefficients are derived from the linearized Boltzmann-BGK equation for Poiseuille flows—i.e., pressure-driven (body-force-driven) flows between two parallel plates.

Cercignani [45] also obtained the asymptotic solution for the normalized mass flux for $\mathrm{Kn} \ll 1$:

$$Q_\delta = \frac{\delta}{u_0 H}\int_0^H u\, dy = \frac{1}{6}\delta + \sigma + \frac{(2\sigma^2 - 1)}{\delta}, \tag{20}$$

where $\sigma = 1.01615$ and u_0 is the centerline velocity for the Navier-Stokes solution with no-slip boundary condition. The rarefaction parameter δ is related to Kn as $\delta = \sqrt{\pi}/(2\mathrm{Kn})$. For consistent comparison with the LB equation, the normalized mass flow rate can be rewritten as

$$Q = \frac{1}{u_0 H \mathrm{Kn}}\int_{-H/2}^{H/2} u\, dy = \frac{1}{6\mathrm{Kn}} + c_1 - (2c_2 + c_3)\mathrm{Kn}, \tag{21}$$

where $c_3 = 0.595\ 16$.

B. Lattice Boltzmann equation and effective diffuse scattering boundary condition

Here, an analytic solution of the D2Q9 LB equation is obtained for Poiseuille flow. Since the LB equation is consistent with the DVB equation when $\delta t \to 0$, the DVB equation will also be referred to as the LB equation, hereafter, for convenience. The discrete lattice effects due to time and spatial discretization will be discussed later in Sec. III E. The solution method is based on that of Ansumali *et al.* [34], where a moment system corresponding to the LB equation is solved. In addition to the conserved moments ρ and j_α, the moment system includes three components of the stress tensor, two components of energy flux, and a scalar fourth-order moment:

$$P_{\alpha\beta} = \sum_i f_i c_{i\alpha} c_{i\beta}, \tag{22}$$

$$q_\alpha = \sum_i f_i c_{i\alpha} c_i^2, \tag{23}$$

$$\Psi = R_{yyyy} + R_{xxxx} - 2R_{xxyy}, \tag{24}$$

where $R_{\alpha\beta\gamma\theta} = \Sigma_i f_i c_{i\alpha} c_{i\beta} c_{i\gamma} c_{i\theta}$. The equations for the moments are derived from the LB equation. Here, only the steps for the derivation of the velocity profile and the slip velocity are presented.

In Poiseuille flow, the flow is steady, $\partial_t(\cdot) = 0$, and unidirectional, $\partial_x(\cdot) = 0$. Under these conditions, the equations for the density and the momentum density can be written as

$$\partial_y j_y = 0, \tag{25}$$

$$\partial_y P_{xy} = \rho g, \tag{26}$$

$$\partial_y (P - N) = 0, \tag{27}$$

where $P = P_{xx} + P_{yy}$ and $N = P_{xx} - P_{yy}$. For impermeable walls, which are located at $y = H/2$ and $-H/2$, we obtain

$$j_y = 0, \tag{28}$$

$$P = N + P_0. \tag{29}$$

From the equations for normal stresses,

$$\partial_y q_y = -\frac{1}{\tau}\left(N - \frac{j_x^2}{\rho}\right), \tag{30}$$

$$\partial_y q_y = \frac{1}{\tau}\left(N + P_0 - 2\rho c_s^2 - \frac{j_x^2}{\rho}\right), \tag{31}$$

we obtain $P_0 = 2\rho c_s^2$, which shows that the density is constant. The shear stress can then be obtained as

$$P_{xy} = \rho g y, \tag{32}$$

where the symmetry of the flow at $y = 0$ is used. The equation of the shear stress reads

$$\partial_y (q_x - 3c_s^2 j_x) = -\frac{1}{\tau} P_{xy}. \tag{33}$$

Using the equation for energy flux q_x,

$$6c_s^2 \partial_y P_{xy} = -\frac{1}{\tau}(q_x - 4c_s^2 j_x) + 4c_s^2 \rho g, \tag{34}$$

the equation for the momentum j_x is finally obtained:

$$\partial_y (-6\tau c_s^2 \partial_y P_{xy} + 4\tau c_s^2 \rho g + c_s^2 j_x) = -\frac{1}{\tau} P_{xy}. \tag{35}$$

Substituting the results for the shear stress and the density, we obtain

$$\partial_y (-2\tau c_s^2 g + c_s^2 u_x) = -\frac{1}{\tau} g y. \tag{36}$$

The differentiation of the above equation gives

$$\partial_y (\nu \partial_y u_x) = -g. \tag{37}$$

For body-force-driven Poiseuille flow, the hydrodynamic equation for the D2Q9 LB equation is the Navier-Stokes equation for all Kn. This is consistent with the previous finding that the analytic solution of the LB method for this flow has a parabolic profile [24].

From Eq. (36), the solution for the velocity u_x can be written as

$$u_x = -\frac{1}{2\nu} g y^2 + 2\nu g + u_0. \tag{38}$$

The integration constant u_0 can be obtained from the boundary condition of the distribution functions. At the bottom wall, the particles are assumed to be reflected diffusely. The diffuse scattering boundary condition is given by

$$f_i|_{y=-H/2} = f_i^{\mathrm{eq}}(\rho, \rho u_{x,w}, \rho u_{y,w}) = \rho w_i, \quad \text{for } i = 2,5,6, \tag{39}$$

where $u_{\alpha,w}$ is the velocity of the wall. The nonequilibrium distribution function at the wall is then given by

$$f_i^{\mathrm{neq}}|_{y=-H/2} = \rho w_i - f_i^{\mathrm{eq}}(\rho, j_x|_{y=-H/2}, 0), \quad \text{for } i = 2,5,6. \tag{40}$$

Using Eq. (40), we obtain

$$[f_5^{\mathrm{neq}} - f_6^{\mathrm{neq}}]_{y=-H/2} = -\frac{\sqrt{3}}{18}\frac{j_x|_{y=-H/2}}{c_s} = -\frac{\sqrt{3}}{18}\frac{\rho}{c_s}\left(-g\frac{H^2}{8\nu} + 2\nu g + u_0\right). \quad (41)$$

Alternatively, the nonequilibrium distribution function can be obtained using the linear relationship between the distribution functions and the moments:

$$f_i^{\mathrm{neq}} = w_i\left[\frac{P_{xy}^{\mathrm{neq}}}{c_s^4}c_{ix}c_{iy} + \frac{q_x^{\mathrm{neq}}}{2c_s^6}(c_{ix}c_i^2 - 4c_s^2c_{ix}) + \frac{q_y^{\mathrm{neq}}}{2c_s^6}(c_{iy}c_i^2 - 4c_s^2c_{iy}) + \frac{N^{\mathrm{neq}}}{2c_s^6}(c_{ix}^2 - c_s^2)c_{iy}^2\right], \quad (42)$$

where the superscript "neq" represents the nonequilibrium part of the quantity. Evaluating Eq. (42) at the bottom wall gives

$$[f_5^{\mathrm{neq}} - f_6^{\mathrm{neq}}]_{y=-H/2} = \frac{P_{xy}^{\mathrm{neq}}|_{y=-H/2}}{6c_s^2} + \frac{\sqrt{3}}{18}\frac{q_x^{\mathrm{neq}}|_{y=-H/2}}{c_s^3} = -\frac{\rho g H}{12c_s^2} - \frac{\sqrt{3}}{18}\frac{2\tau c_s^2 \rho g}{c_s^3}. \quad (43)$$

Comparing Eqs. (41) and (43) we obtain

$$u_0 = g\left(\frac{\sqrt{3}H}{2c_s} + \frac{H^2}{8\tau c_s^2}\right). \quad (44)$$

The normalized velocity is thus given by

$$\hat{u}_x = -\left(\frac{y}{H}\right)^2 + \frac{1}{4} + \sqrt{\frac{6}{\pi}}\mathrm{Kn} + \frac{8}{\pi}\mathrm{Kn}^2, \quad (45)$$

where $\hat{u}_x = 2\nu/(gH^2)u_x$. For D2Q9, the first-order and second-order slip coefficients are therefore $c_{1,9} = \sqrt{6/\pi}$ and $c_{2,9} = 4/\pi$, respectively, and the normalized mass flow rate is given by

$$Q = \frac{1}{6\mathrm{Kn}} + \sqrt{\frac{6}{\pi}} + \frac{8}{\pi}\mathrm{Kn}. \quad (46)$$

The present analysis is based on the second-order equilibrium and forcing terms, Eqs. (2) and (3). For body-force-driven Poiseuille flows, however, the second-order terms in Eqs. (2) and (3) are only concerned with the normal stress N and the nonequilibrium distributions. For the straight walls parallel to the main axis of the lattice velocities, the slip velocity and the velocity profile are, therefore, identical to those obtained using the Stokes equilibrium and the linear forcing term given by

$$f_i^{\mathrm{eq}} = w_i\left(\rho + \frac{j_\alpha c_{i\alpha}}{c_s^2}\right), \quad (47)$$

$$F_i = w_i\rho\frac{g_\alpha c_{i\alpha}}{c_s^2}. \quad (48)$$

The slip (and bulk) velocity can be affected by the second-order terms for inclined channels and general flows.

The slip coefficients for the D2Q9 LB equation are higher than those for the linearized Boltzmann equation. This is the result of the discretization in velocity space. To obtain a correct value of the slip coefficient, the *effective* diffuse scattering condition can be introduced by combining the diffuse scattering boundary condition and the bounce-back scheme:

$$f_i = rf_i^b + (1-r)f_i^d, \quad (49)$$

where the superscripts b and d represent the bounce-back scheme and the diffuse scattering boundary condition, respectively, and r is the fraction of fluid particles reflected with the bounce-back rule. For the boundary condition of Eq. (49), the integration constant u_0 is given by

$$u_0 = g\left(\frac{1-r}{1+r}\frac{\sqrt{3}H}{2c_s} + 2\tau + \frac{H^2}{8\tau c_s^2}\right). \quad (50)$$

The normalized velocity and the normalized mass flux are thus given by

$$\hat{u}_x = -\left(\frac{y}{H}\right)^2 + \frac{1}{4} + \frac{1-r}{1+r}\sqrt{\frac{6}{\pi}}\mathrm{Kn} + \frac{8}{\pi}\mathrm{Kn}^2, \quad (51)$$

$$Q = \frac{1}{6\mathrm{Kn}} + \frac{1-r}{1+r}\sqrt{\frac{6}{\pi}} + \frac{8}{\pi}\mathrm{Kn}. \quad (52)$$

The introduction of the bounce-back scheme influences only the first-order slip coefficient. In the analysis of the boundary condition in the LB model, the bounce-back scheme is known to give second-order slip velocity in Kn [10,26]. Equation (51) shows that this second-order slip velocity occurs regardless of the spatial and temporal discretization, and that the bounce-back scheme has the same second-order slip coefficient as the diffuse scattering boundary condition. In the D2Q9 LB equation for Poiseuille flow, the second-order slip velocity is induced by the nonequilibrium energy flux q_x^{neq}. In Couette flow, where the nonequilibrium energy flux vanishes, the bounce-back scheme produces a no-slip condition for all Kn. In what follows, two methods to adjust the second-order slip coefficient are presented.

C. Modification of energy flux in the lattice Boltzmann equation

According to the present analysis, the second-order slip coefficient in the D2Q9 LB equation can be adjusted by modifying the energy flux in the moment system. This can be achieved by the modified LB equation

$$\partial_t f_i + c_{i\alpha}\partial_\alpha f_i = -\frac{1}{\tau}(f_i - f_i^{\mathrm{eq}}) + F_i + S_i, \quad (53)$$

where

$$S_i = -r_q\frac{w_i}{\tau}\left[\frac{q_x^{\mathrm{neq}}}{2c_s^6}(c_{ix}c_i^2 - 4c_s^2c_{ix}) + \frac{q_y^{\mathrm{neq}}}{2c_s^6}(c_{iy}c_i^2 - 4c_s^2c_{iy})\right]. \quad (54)$$

For Poiseuille flow, the energy flux q_x^{neq} then becomes

$$q_x^{\mathrm{neq}} = -2\tau_q c_s^2 \rho g, \tag{55}$$

where $\tau_q = \tau/(1+r_q)$. With the modified energy flux q_x^{neq}, the normalized velocity and the normalized mass flux are given by

$$\hat{u}_x = -\left(\frac{y}{H}\right)^2 + \frac{1}{4} + \frac{1-r}{1+r}\sqrt{\frac{6}{\pi}}\mathrm{Kn} + \frac{1}{1+r_q}\frac{8}{\pi}\mathrm{Kn}^2, \tag{56}$$

$$Q = \frac{1}{6\mathrm{Kn}} + \frac{1-r}{1+r}\sqrt{\frac{6}{\pi}} + \frac{1}{1+r_q}\frac{8}{\pi}\mathrm{Kn}. \tag{57}$$

The second-order discrete form of the modified LB equation can be written as

$$\hat{f}_i(\mathbf{x}+\delta t\mathbf{c}_i, t+\delta t) - \hat{f}_i(\mathbf{x},t) = -\frac{\delta t}{\tau+\delta t/2}(\hat{f}_i - f_i^{\mathrm{eq}}) + \frac{\tau}{\tau+\delta t/2}(F_i+S_i)\delta t. \tag{58}$$

From the transformation $\hat{f}_i = f_i - (\Omega_i + S_i)\delta t/2$ and the moment relations, the noneqilibrium energy flux is given by

$$q_\alpha^{\mathrm{neq}} = \frac{1}{1+\delta t/(2\tau_q)}\left(\sum_i c_{i\alpha}c_i^2\hat{f}_i - 4c_s^2\sum_i c_{i\alpha}\hat{f}_i\right). \tag{59}$$

Sbragaglia and Succi [26] suggested to modify the construction of the body force in the LB model in order to adjust the second-order slip coefficient. This is possible when selecting the direction of the body force parallel to one of the lattice velocities— e.g., $c_{1\alpha}$. By releasing the isotropy requirement for the body-force term, free parameters are obtained, which can be used to adjust the second-order slip coefficient. Essentially, their method corresponds to a modification of the energy flux q_x. However, the method of Sbragaglia and Succi can be applied only when flows are driven by a body force, while the present method can be applied to pressure-driven flows.

In the MRT model [22,23], the different relaxation times can be independently adjusted to overcome the limitations of the BGK model—for example, numerical stability. The slip velocity in the MRT model is also shown to depend on the relaxation times for third-order moments [25,31]. The present analysis shows that the slip velocity at second order in Kn is specifically related to the nonequlibrium energy flux mode, which is consistent with the previous results for the MRT model [20,25]. In Eq. (53), the nonequilibrium energy flux is effectively adjusted by adding a source term to the LB-BGK equation.

D. Lattice Boltzmann equation with the effective relaxation time

In the Knudsen layer or kinetic boundary layer [45], an average distance traveled by molecules before collisions—i.e., the mean free path—is smaller than that in homogeneous bulk fluid due to the presence of the wall boundary. As a result, the hydrodynamic momentum transfer is different from that in the bulk fluid and the Navier-Stokes hydrodynamics or the linear relationship of the stress and the strain is invalid in this layer with thickness of the order of the mean free path. Guo *et al.* [33] argued that the relaxation time in the BGK model should also be changed according to changes in the mean free path in the confined geometry and proposed to use a relaxation time that accounts for wall confinement effects in the LB method. Zhang *et al.* [27] also proposed an effective mean free path, with the same physical picture as Guo *et al.* [33], but considered the variation of the effective mean free path along the wall normal direction.

While the arguments of Guo *et al.* [33] and Zhang *et al.* [27] on the effective mean free path are physically sound, the implication on the relaxation time in the BGK model is worthwhile to discuss. In Guo *et al.* [33] and Zhang *et al.* [27], the effective relaxation time is given by $\tau_e = \lambda_e/c$, where τ_e and λ_e are the effective relaxation time and the effective mean free path, respectively, and c is a properly chosen mean molecular speed. The confinement effects contained in the effective mean free path are entirely transferred to the effective relaxation time.

In the Boltzmann-BGK equation, particles can have all allowable ranges of velocities. During the time interval of the order of the relaxation time, particles with velocities larger than H/τ interact with the wall before relaxing to the local-equilibrium even in relatively homogeneous hydrodynamic field. The effects of the wall confinement appear therefore in the solution of the Boltzmann-BGK equation even with a fixed relaxation time that is determined by the bulk fluid viscosity. This can be easily verified by the fact that the solution of the linearized Boltzmann-BGK equation, with fixed relaxation time, agrees excellently with that of the DSMC method [46] in simple flows for all Kn. Therefore, in the Boltzmann-BGK equation, the relaxation time represents the intrinsic property of molecules and there is no need to modify the relaxation time to consider the geometric effects such as the wall confinement.

This argument suggests that the concept of effective relaxation time is restricted to a reduced-order model of the Boltzmann-BGK equation. In addition, a specific relation between the effective relaxation time and the effective mean free path depends on the reduced-order model for which it is applied. In the LB method, the velocity space is represented by a finite number of discrete velocities and each discrete distribution function represents a group of particles with a range of velocities. In the D2Q9 LB method, in particular, all particles move with the same wall normal velocity and relax to the local equilibrium with the same relaxation time. In contrast to the continuum Boltzmann-BGK equation, the effects of the wall confinement on the relaxation dynamics are the same for all particles in D2Q9. This is perhaps the reason why the Knudsen layer is not captured in D2Q9. In hydrodynamics, the effects of the wall boundary on the momentum transfer in the Knudsen layer can be represented by the effective viscosity [47]

$$\nu_e = -\frac{1}{\rho}\frac{P_{xy}}{\partial_y u_x}. \tag{60}$$

Since the macroscopic equation for the D2Q9 LB model is the Navier-Stokes equation for all Kn, the effective relaxation time is defined as

$$\tau_e = \frac{\nu_e}{c_s^2}. \tag{61}$$

This is equivalent to the relation between the effective relaxation time and the effective mean free path in Guo *et al.* [33] and Zhang *et al.* [27].

Here, we analyze the effective relaxation time model using an exact solution. The effective relaxation time is assumed to be

$$\tau_e = \frac{\tau}{1 + a\psi}, \tag{62}$$

where

$$\psi = (1 - I)\exp\left[-\frac{b}{\mathrm{Kn}}\left(\frac{y}{H} + \frac{1}{2}\right)\right] + I\exp\left[\frac{b}{\mathrm{Kn}}\left(\frac{y}{H} - \frac{1}{2}\right)\right]. \tag{63}$$

The indicator function I is zero for $y < 0$ and unity for $y \geq 0$. For the effective diffuse scattering condition, the normalized velocity and mass flux are given by

$$\hat{u}_x = -\left(\frac{y}{H}\right)^2 + \frac{1}{4} + \left[\sqrt{\frac{6}{\pi}}\frac{1-r}{1+r} + \frac{a}{b}\left(1 - 2\frac{y}{H}\phi\right)\right]\mathrm{Kn} + 2\left[\frac{4}{\pi(1+a\psi)} - \frac{a}{b^2}(1-\psi)\right]\mathrm{Kn}^2, \tag{64}$$

$$Q = \frac{1}{6\mathrm{Kn}} + \left(\sqrt{\frac{6}{\pi}}\frac{1-r}{1+r} + \frac{a}{b}\right) + \left[\frac{8}{\pi} - 4\frac{a}{b^2}\right]\mathrm{Kn} + Q_h, \tag{65}$$

where

$$\phi = -(1 - I)\exp\left[-\frac{b}{\mathrm{Kn}}\left(\frac{y}{H} + \frac{1}{2}\right)\right] + I\exp\left[\frac{b}{\mathrm{Kn}}\left(\frac{y}{H} - \frac{1}{2}\right)\right], \tag{66}$$

$$Q_h = 8\left[\frac{a}{b^3}(1 - e^{-b/(2\mathrm{Kn})}) - \frac{2}{\pi}\frac{\ln(1+a) - \ln(1 + ae^{-b/(2\mathrm{Kn})})}{b}\right]\mathrm{Kn}^2. \tag{67}$$

There are two effects due to the effective relaxation time: the decrease of the overall flow resistance in the bulk fluid due to the decreased viscosity near the walls and the decrease of the slip velocity due to the decrease in the relaxation time. The former effect first appears in the first-order term in Kn, while the latter effect appears in the second- and higher-order terms in Kn. With $a/b > 0$, the effective relaxation time introduces additional first-order slip in Kn. To match the first-order slip coefficient, the parameter r in the effective diffuse scattering boundary condition should thus be adjusted accordingly.

E. Discrete lattice effects in the boundary condition and slip velocity

The analytic solutions for the slip velocity are obtained for the DVB equation. Due to finite lattice spacing, the slip velocity in the LB method involves the discretization error or discrete lattice effects [39]. The LB equation (10) is obtained from the second-order implicit time integration of the DVB equation, and thus the discretization error in fluid lattices is of $O(\delta^2)$, where $\delta = H/N$ is the lattice spacing. For the boundary closure, the halfway scheme is used to obtain second-order accuracy for a straight wall [19,20,24]. In the transverse direction, fluid lattices are indexed from 1 to N, while the boundary lattices are 0 and $N+1$. For the wall boundary located at $y = -H/2$, the boundary lattices are located at $y = -H/2 - \delta/2$, while the boundary lattices are located at $y = H/2 + \delta/2$ for the upper wall. After the propagation step, the unknown distribution functions at the wall boundary lattices are given by

$$\hat{f}_i = r\hat{f}_i^b + (1 - r)f_i^d. \tag{68}$$

To get some insights into discrete lattice effects in the boundary closure, it is instructive to discuss the bounce-back scheme for which the analytic solution of the slip velocity is known [24,25]. From Eq. (43) of He *et al.* [24], the slip velocity for the (halfway) bounce back scheme is given by

$$u_s^e = u_c\frac{[4\tau^*(4\tau^* - 5) + 3]}{3N^2}, \tag{69}$$

where $u_c = H^2 g/(8\nu)$ and $\tau^* = \bar{\tau} + 1/2$. $\bar{\tau}$ is the relaxation time in the lattice unit. Equation (69) is derived for the explicit treatment of the linear part of the external force term. For the normalized slip velocity we obtain

$$\hat{u}_s^e = 4\frac{[(\bar{\tau} + 1/2)(\bar{\tau} - 3/4) + 3/16]}{3N^2} = \frac{8}{\pi}\mathrm{Kn}^2 - \sqrt{\frac{2}{3\pi}}\mathrm{Kn}\frac{1}{N} - \frac{1}{4N^2}, \tag{70}$$

where $\hat{u}_s^e = 2\nu/(H^2 g)u_s^e$.

In Eq. (70), the physical slip velocity, which does not vanish as $\delta \to 0$ for a given Kn, is equal to that in Eq. (51) with $r = 1$. However, the (halfway) bounce-back scheme with the explicit treatment of the forcing term has a spurious slip velocity at first order in Kn. This spurious slip velocity is of first order in δ. In the second-order implicit treatment of the external force term, the normalized slip velocity is given by

$$\hat{u}_s = \hat{u}_s^e + \frac{g}{2}\frac{2\nu}{H^2 g} = \frac{8}{\pi}\mathrm{Kn}^2 - \frac{1}{4N^2}. \tag{71}$$

Note that the spurious first-order term is removed in Eq. (71) and the scheme is of second order in δ.

For the modified LB equation with the effective diffuse scattering boundary condition, the normalized slip velocity with discrete lattice effects is found to be

$$\hat{u}_s = \frac{1-r}{1+r}\sqrt{\frac{6}{\pi}}\mathrm{Kn} + \frac{1}{1+r_q}\frac{8}{\pi}\mathrm{Kn}^2 - \frac{1}{4N^2}. \tag{72}$$

The discretization error is identical to that for the (halfway) bounce-back scheme. The problem of discrete effects in the kinetic boundary condition has also been addressed in Guo *et al.* [48].

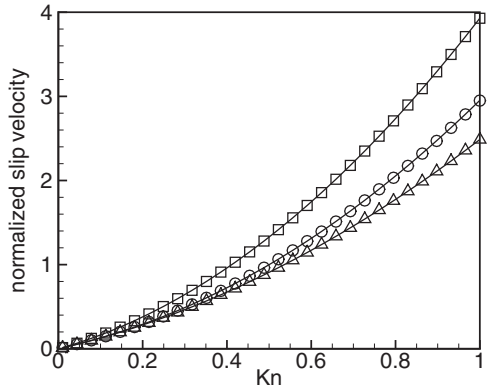

FIG. 1. Normalized slip velocity u_s for Poiseuille flow. The slip velocity is defined as $u_s = Q\mathrm{Kn} - 1/6$. Numerical solutions for D2Q9 (squares), D2Q9EDQ (triangles), and D2Q9EDT (circles) are compared with analytic solutions (lines).

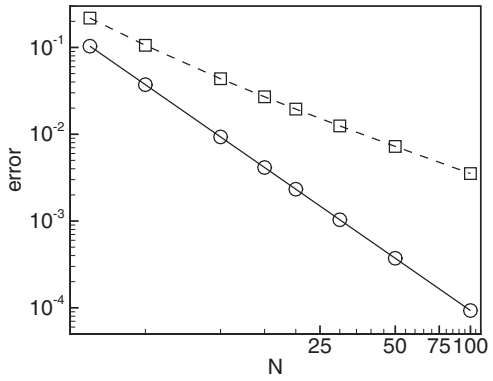

FIG. 2. Discretization errors of the slip velocity, defined by Eq. (73), for D2Q9 with the (halfway) bounce-back scheme. The LB equation with the second-order implicit time integration (circles) is a second-order scheme, while that with the explicit treatment of the external body-force term (squares) is a first-order scheme. The numerical simulation results exactly match with the analytic solutions, Eqs. (70) (dashed line) and (71) (solid line).

IV. NUMERICAL SIMULATIONS

Numerical simulations using the proposed LB methods were performed for Poiseuille and Couette flows. Hereafter, the D2Q9 scheme with the effective diffuse scattering boundary condition is referred to as D2Q9ED, the D2Q9 scheme with the effective diffuse scattering boundary condition and the modified energy flux term is referred to as D2Q9EDQ, and the D2Q9 scheme with the effective diffuse scattering boundary condition and the effective relaxation time is referred to as D2Q9EDT. For D2Q9ED, the parameter r is set to give the exact first-order slip coefficient c_1. For D2Q9EDQ, r_q is set to 0.9 in order to match the normalized mass flow rate for the linearized Boltzmann equation to second order in Kn. For D2Q9EDQ, $a=0.3$ and $b=1$, and r is set to give the exact first-order slip coefficient c_1. To assess the new models, for both Poiseuille and Couette flows, solutions are compared with results obtained using the DSMC method [46]. The DSMC method is a particle method for rarefied gas flows that performs a direct simulation of the physics in the full Boltzmann equation. The DSMC method is often used in studies of microscale gas flows to evaluate more approximate, more numerically efficient techniques [27,34,49].

A. Poiseuille flow

Analytic solutions for the normalized slip velocity are compared with results from numerical simulations in Fig. 1. The slip velocity here is defined as $u_s = Q\mathrm{Kn} - 1/6$. The analytic solutions are in excellent agreement with the numerical results. In numerical simulations, the periodic condition is used for the streamwise direction, while the (effective) diffuse scattering boundary condition is used on the walls. The transverse direction is discretized into 53 grid points including the boundary points.

Figure 2 shows the discretization errors for the slip velocity for D2Q9 with the (halfway) bounce-back scheme. The error is defined by

$$\epsilon = \frac{\hat{u}_s^{\mathrm{DVB}} - \hat{u}_s^{\mathrm{LB}}}{\hat{u}_s^{\mathrm{DVB}} + 1/6}, \tag{73}$$

where $\hat{u}_s^{\mathrm{DVB}}$ and $\hat{u}_s^{\mathrm{LB}}$ are the normalized slip velocity for the DVB equation and for the LB equation, respectively. The numerical simulation results exactly match with the analytic solutions, Eqs. (70) and (71). This confirms the analysis in Sec. III E: For the LB equation with the (halfway) bounce-back scheme, second-order implicit time integration results in a second-order scheme, while an explicit treatment of the external body-force term results in a first-order scheme. Figure 3 shows the discretization errors for the slip velocity for D2Q9EDQ. The discretization errors from the numerical simulations exactly match with those for Eq. (72).

Figure 4 shows the normalized mass flow rate Q. The normalized mass flow rates predicted by various LB methods are compared with the linearized Boltzmann [50] and DSMC solutions for a range of Kn. DSMC solutions agree well with those of the linearized Boltzmann equation for the range of

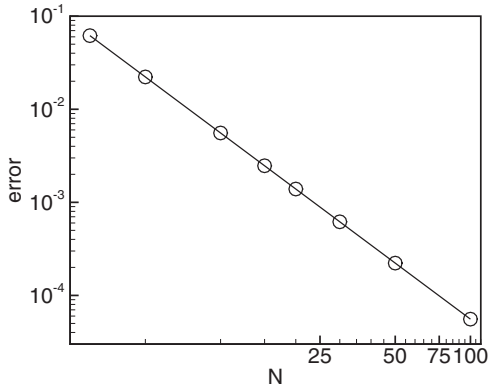

FIG. 3. Discretization errors of the slip velocity, defined by Eq. (73), for D2Q9EDQ. The discretization errors from the numerical simulations (circles) exactly match with those for Eq. (72) (line).

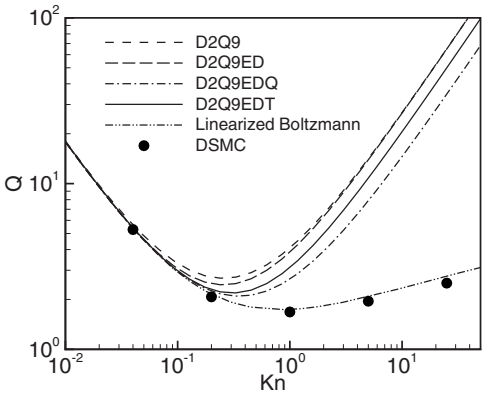

FIG. 4. Normalized mass flow rate for Poiseuille flow. The normalized mass flow rate is defined by $Q=1/(u_0H\mathrm{Kn})\int_{-H/2}^{H/2}u\,dy$, where u_0 is the maximum velocity for the Navier-Stokes equation with no-slip boundary condition.

Kn considered here, which supports the argument on the relaxation time in the previous section. D2Q9 well predicts a mass flow rate up to about $\mathrm{Kn}\approx 0.05$. For D2Q9ED with an accurate first-order slip coefficient, the range of Kn that is in quantitative agreement with the reference solutions extends to about $\mathrm{Kn}\approx 0.1$. With improved second-order slip coefficients, D2Q9EDQ and D2Q9EDT agree well with the DSMC method and linearized Boltzmann equation also for the moderate transition regime—i.e., $\mathrm{Kn}\approx 0.2-0.3$. For $\mathrm{Kn}>0.5$, D2Q9EDT predicts slightly higher Q than D2Q9EDQ due to the higher-order term Q_h in Eq. (65). All LB methods predict the Knudsen minimum due to the second-order and higher-order slip components.

Figure 5 shows the streamwise velocity profiles at $\mathrm{Kn}=0.04$ and $\mathrm{Kn}=0.2$. The velocity is normalized using the bulk mean velocity $u_b=\int_{-H/2}^{H/2}u\,dy/H$. At $\mathrm{Kn}=0.04$, all LB methods are in very good agreement with the DSMC method. At $\mathrm{Kn}=0.2$, D2Q9 and D2Q9EDQ overpredict the velocity near walls, and the velocity profile is flatter than that of the DSMC method, while D2Q9EDT is in good agreement with the DSMC method. Considering the mass flow rate is well predicted by D2Q9EDQ, the flatter velocity profile predicted by D2Q9EDQ is due to its lack of capturing the Knudsen layer.

B. Couette flow

The proposed LB methods with the same set of model constants are applied to planar Couette flow. In the planar Couette flow, the top plate at $y=H/2$ moves with velocity U, while the bottom plate at $y=-H/2$ moves with velocity $-U$. The periodic condition is used for the streamwise direction, while the (effective) diffuse scattering boundary condition is used on the walls. The transverse direction is discretized into 53 grid points including the boundary points.

Figure 6 shows the streamwise velocity profiles for $\mathrm{Kn}=0.1$, 0.25, 0.5, and 1. The discrepancy between the D2Q9 and DSMC approaches increases with Kn, while D2Q9EDQ improves D2Q9 only slightly. D2Q9EDT, however, gives significantly improved results for $\mathrm{Kn}<1$. The nonlinear profile in the Knudsen layer in DSMC is also captured by D2Q9EDT, as reported in Zhang *et al.* [27]. In Zhang *et al.* [27], with the model constant a in D2Q9EDT being 0.7 and with the diffuse scattering boundary condition, they obtained very good results for Couette flow. However, as in Eq. (65), without modifying the boundary condition, D2Q9EDT gives higher mass flow rate in Poiseuille flow than D2Q9.

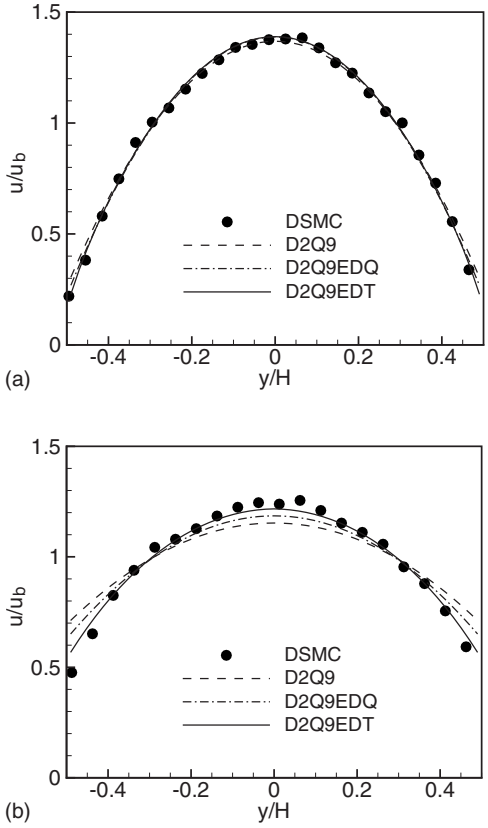

FIG. 5. Distribution of the streamwise velocity for (a) $\mathrm{Kn}=0.04$ and (b) $\mathrm{Kn}=0.2$ in Poiseuille flow. The velocity is normalized by $u_b=\int_{-H/2}^{H/2}u\,dy/H$.

Figure 7 shows the actual slip velocity at the wall, $(u_w-u_f)/u_w$, where u_w and u_f are the velocity of the wall and the fluid velocity at the wall, respectively, and the slip velocity measured using the velocity gradient at the centerline, $1-(du_x/dy)|_{y=0}/(2U)$. D2Q9 overpredicts the actual slip even at very small Kn, while the slip velocity based on the velocity gradient at the centerline is in good agreement with the linearized Boltzmann solution [51] for $\mathrm{Kn}<0.05$. This is because D2Q9 does not capture the Knudsen layer. In Couette flow, since the nonequilibrium energy flux q_x^{neq} vanishes, only first-order slip in Kn appears for D2Q9 and D2Q9EDQ is equivalent to D2Q9ED. By improving the first-order slip coefficient, D2Q9ED(Q) accurately predicts the slip velocity based on the velocity gradient at the centerline up to $\mathrm{Kn}\approx 0.15$. D2Q9EDT agrees well with the linearized Boltzmann equation for the range of Kn considered here.

V. CONCLUSIONS

Lattice Boltzmann models that can predict slip velocity up to second order in the Knudsen number are presented. The

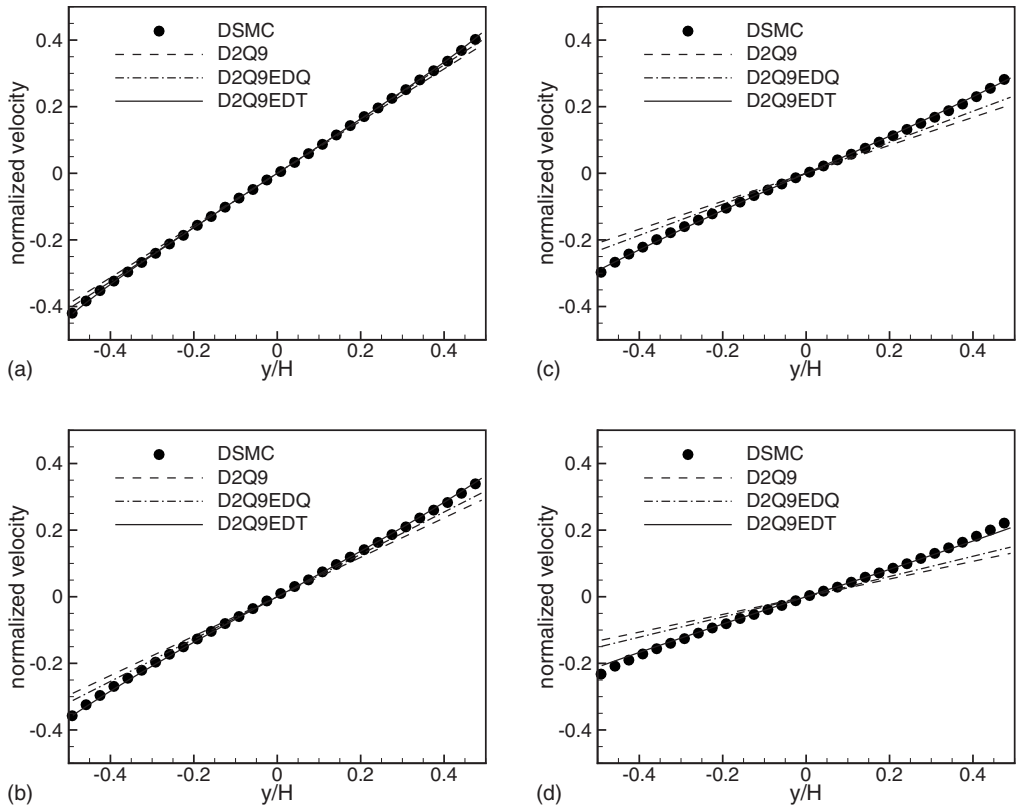

FIG. 6. Distribution of the streamwise velocity for (a) Kn=0.1, (b) Kn=0.25, (c) Kn=0.5, and (d) Kn=1 in Couette flow. The velocity is normalized by the difference between the velocities of the top and bottom plates.

exact solution of the slip velocity for the LB equation is obtained for Poiseuille flow at finite Kn. With a consistent definition of the Kn, the slip coefficients of the LB equation with the standard D2Q9 scheme are found to be slightly larger than those of the Boltzmann equation with the same boundary condition, which causes the D2Q9 LB method to remain quantitatively accurate only for small Kn. The effective diffuse scattering boundary condition is introduced to reproduce the first-order slip coefficient in the asymptotic solution of the Boltzmann equation. It is found that the second-order slip velocity in the D2Q9 LB method is related to the nonequilibrium energy flux, which is consistent with the previous results for the MRT model. A modified LB equation is proposed, which has a source term to modify the nonequilibrium energy flux and thus has an adjusted second-order slip coefficient. To capture the Knudsen layer, the LB method with the effective relaxation time is proposed and analyzed with the exact solution. With the effective relaxation time and the effective diffuse scattering boundary condition, the slip flow is predicted up to second order in Kn and the Knudsen layer is captured. For the standard LB method, the Knudsen layer is captured only with the modification of the relaxation dynamics as in the effective relaxation time model.

The present analysis is restricted to straight walls. For application to flows in complex geometry, a boundary closure based on an interpolation method [25,52] can be utilized to minimize errors due to finite lattice spacing. Another issue is the anisotropy of the slip velocity. In Cornubert *et al.* [19] and Ginzburg and Alder [20], the slip velocity is shown to be anisotropic with respect to the orientation of the wall boundary. The analysis of the slip velocity in flows with curved streamlines is also an open problem.

ACKNOWLEDGMENTS

Financial support by Honda R&D Co., Ltd. Fundamental Technology Research Center, Wako Research Center, is gratefully acknowledged. I.D.B. expresses his gratitude to Stanford University for partial support during a sabbatical leave.

APPENDIX

For Poiseuille flow, the equation for u_x for the D2Q9 scheme with effective relaxation time can be written as

$$\partial_y(-2\tau_e c_s^2 g + c_s^2 \rho u_x) = -\frac{1}{\tau_e} g y. \tag{A1}$$

The effective relaxation time is assumed to be

$$\tau_e = \frac{\tau}{1 + a\psi},$$

where

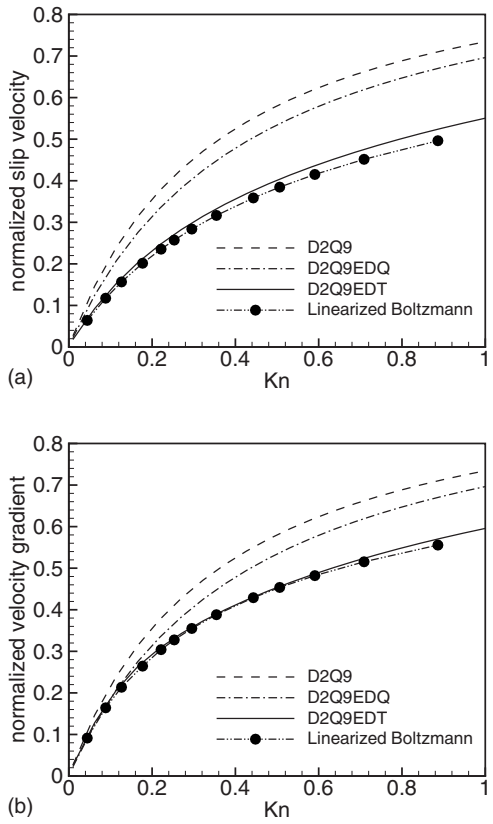

FIG. 7. Normalized slip velocity in Couette flow. (a) actual slip velocity $(u_w-u_f)/u_w$, where u_w and u_f are the velocity of the wall and the fluid velocity at the wall, respectively, and (b) the slip velocity measured using the velocity gradient at the centerline, $1-(du_x/dy)|_{y=0}/(2U)$.

$$\psi = (1-I)\exp\left[-\frac{b}{\mathrm{Kn}}\left(\frac{y}{H}+\frac{1}{2}\right)\right] + I\exp\left[\frac{b}{\mathrm{Kn}}\left(\frac{y}{H}-\frac{1}{2}\right)\right].$$

The indicator function I is zero for $y<0$ and unity for $y \geq 0$. The solution for u_x then reads

$$u_x = -\frac{1}{2\nu}gy^2 + u_0 + 2\tau_e g - \frac{ag}{\tau c_s^2}\frac{H}{b}y\phi\mathrm{Kn} + \frac{ag}{\tau c_s^2}\frac{H^2}{b^2}\psi\mathrm{Kn}^2, \tag{A2}$$

where

$$\phi = -(1-I)\exp\left[-\frac{b}{\mathrm{Kn}}\left(\frac{y}{H}+\frac{1}{2}\right)\right] + I\exp\left[\frac{b}{\mathrm{Kn}}\left(\frac{y}{H}-\frac{1}{2}\right)\right].$$

For the combination of the diffuse scattering and bounce-back boundary condition,

$$f_i = rf_i^b + (1-r)f_i^d,$$

we obtain

$$[f_5^{\mathrm{neq}} - f_6^{\mathrm{neq}}]_{y=-H/2} = r[f_7^{\mathrm{neq}} - f_8^{\mathrm{neq}}]_{y=-H/2} - (1+r)\frac{\sqrt{3}}{18}\frac{j_x|_{y=-H/2}}{c_s}$$
$$= r\left(\frac{P_{xy}^{\mathrm{neq}}|_{y=-H/2}}{6c_s^2} - \frac{\sqrt{3}}{18}\frac{q_x^{\mathrm{neq}}|_{y=-H/2}}{c_s^3}\right)$$
$$-(1+r)\frac{\sqrt{3}}{18}\frac{j_x|_{y=-H/2}}{c_s}. \tag{A3}$$

The nonequilibrium stress and energy flux are given by $P_{xy}^{\mathrm{neq}}=\rho g y$ and $q_x^{\mathrm{neq}}=2\tau_e c_s^2 \rho g$, respectively. From the linear relationship between the nonequilibrium distribution function and moments, Eq. (42), we obtain

$$[f_5^{\mathrm{neq}} - f_6^{\mathrm{neq}}]_{y=-H/2} = \frac{P_{xy}^{\mathrm{neq}}|_{y=-H/2}}{6c_s^2} + \frac{\sqrt{3}}{18}\frac{q_x^{\mathrm{neq}}|_{y=-H/2}}{c_s^3}$$
$$= -\frac{\rho g H}{12c_s^2} - \frac{\sqrt{3}}{9}\frac{\tau_e \rho g}{c_s}. \tag{A4}$$

Comparing Eqs. (A3) and (A4), we obtain

$$u_0 = g\left[\frac{1-r}{1+r}\frac{\sqrt{3}H}{2c_s} + \frac{H^2}{8\tau c_s^2} - \frac{aH^2}{2b\tau c_s^2}\phi|_{y=-H/2}\mathrm{Kn} - \frac{aH^2}{b^2\tau c_s^2}\psi|_{y=-H/2}\mathrm{Kn}^2\right]. \tag{A5}$$

The normalized velocity and mass flow rate are thus given by

$$\hat{u}_x = -\left(\frac{y}{H}\right)^2 + \frac{1}{4} + \left[\sqrt{\frac{6}{\pi}}\frac{1-r}{1+r} + \frac{a}{b}\left(1-2\frac{y}{H}\phi\right)\right]\mathrm{Kn} + 2\left[\frac{4}{\pi(1+a\psi)} - \frac{a}{b^2}(1-\psi)\right]\mathrm{Kn}^2,$$

$$Q = \frac{1}{6\mathrm{Kn}} + \left(\sqrt{\frac{6}{\pi}}\frac{1-r}{1+r} + \frac{a}{b}\right) + \left[\frac{8}{\pi} - 4\frac{a}{b^2}\right]\mathrm{Kn} + Q_h,$$

where

$$Q_h = 8\left[\frac{a}{b^3}(1-e^{-b/(2\mathrm{Kn})}) - \frac{2}{\pi}\frac{\ln(1+a) - \ln(1+ae^{-b/(2\mathrm{Kn})})}{b}\right]\mathrm{Kn}^2.$$

To obtain (A2) and the normalized mass flow rate Q, the following formulas are used:

$$\int y\psi\, dy = \frac{H}{b}\mathrm{Kn}y\phi - \left(\frac{H}{b}\mathrm{Kn}\right)^2\psi, \tag{A6}$$

$$\int_{-H/2}^{H/2} y\phi\, dy = \frac{H^2}{b}\mathrm{Kn} - 2\left(\frac{H}{b}\mathrm{Kn}\right)^2(1-e^{-b/(2\mathrm{Kn})}), \tag{A7}$$

$$\int_{-H/2}^{H/2}\frac{1}{1+a\psi}dy = H - 2\frac{H}{b}\mathrm{Kn}[\ln(1+a) + \ln(1+ae^{-b/(2\mathrm{Kn})})]. \tag{A8}$$

[1] G. K. Batcheolor, *An Introduction to Fluid Dynamics* (Cambridge University Press, Cambridge, England, 1967).
[2] C.-M. Ho and Y.-C. Tai, Annu. Rev. Fluid Mech. **30**, 579 (1998).
[3] N. G. Hadjiconstantinou, Phys. Fluids **18**, 111301 (2006).
[4] M. Knudsen, Ann. Phys. **333**, 75 (1909).
[5] G. R. McNamara and G. Zanetti, Phys. Rev. Lett. **61**, 2332 (1988).
[6] Y. H. Qian, D. d'Humieres, and P. Lallemand, Europhys. Lett. **17**, 479 (1992).
[7] S. Chen and G. D. Doolen, Annu. Rev. Fluid Mech. **30**, 329 (1998).
[8] R. Benzi, S. Succi, and M. Vergassola, Phys. Rep. **222**, 145 (1992).
[9] S. Succi, *Lattice Boltzmann Equation for Fluid Dynamics and Beyond* (Clarendon Press, Oxford, 2001).
[10] X. B. Nie, G. D. Doolen, and S. Y. Chen, J. Stat. Phys. **107**, 279 (2002).
[11] C. Y. Lim, C. Shu, X. D. Niu, and Y. T. Chew, Phys. Fluids **14**, 2299 (2002).
[12] S. Ansumali and I. V. Karlin, Phys. Rev. E **66**, 026311 (2002).
[13] F. Toschi and S. Succi, Europhys. Lett. **69**, 549 (2005).
[14] S. Ansumali, I. V. Karlin, C. E. Frouzakis, and K. B. Boulouchos, Physica A **359**, 289 (2006).
[15] T. Lee and C.-L. Lin, Phys. Rev. E **71**, 046706 (2005).
[16] V. Sofonea and R. F. Sekerka, J. Comput. Phys. **207**, 639 (2005).
[17] R. Zhang, X. Shan, and H. Chen, Phys. Rev. E **74**, 046703 (2006).
[18] B. Li and D. Y. Kwok, Phys. Rev. Lett. **90**, 124502 (2003).
[19] R. Cornubert, D. d'Humieres, and D. Levermore, Physica D **47**, 241 (1991).
[20] I. Ginzburg and P. M. Adler, J. Phys. II **4**, 191 (1994).
[21] F. J. Higuera, S. Succi, and R. Benzi, Europhys. Lett. **9**, 345 (1989).
[22] P. Lallemand and L.-S. Luo, Phys. Rev. E **61**, 6546 (2000).
[23] D. d'Humières, I. Ginzburg, M. Krafczyk, P. Lallemand, and L.-S. Luo, Philos. Trans. R. Soc. London, Ser. A **360**, 437 (2002).
[24] X. He, Q. Zou, L.-S. Luo, and M. Dembo, J. Stat. Phys. **87**, 115 (1997).
[25] I. Ginzburg and D. d'Humieres, Phys. Rev. E **68**, 066614 (2003).
[26] M. Sbragaglia and S. Succi, Phys. Fluids **17**, 093602 (2005).
[27] Y.-H. Zhang, X. J. Gu, R. W. Barber, and D. R. Emerson, Phys. Rev. E **74**, 046704 (2006).
[28] S. Succi, Phys. Rev. Lett. **89**, 064502 (2002).
[29] G. H. Tang, W. Q. Tao, and Y. He, Phys. Fluids **17**, 058101 (2005).
[30] L. Szalmas, Phys. Rev. E **73**, 066710 (2006).
[31] L. Szalmas, Physica A **379**, 401 (2007).
[32] V. Sofonea and R. F. Sekerka, J. Comput. Phys. **207**, 639 (2005).
[33] Z. Guo, T. S. Zhao, and Y. Shi, J. Appl. Phys. **99**, 074903 (2006).
[34] S. Ansumali, I. V. Karlin, S. Arcidiacono, A. Abbas, and N. Prasianakis, Phys. Rev. Lett. **98**, 124502 (2007).
[35] X. Shan, X.-F. Yuan, and H. Chen, J. Fluid Mech. **550**, 413 (2006).
[36] M. Sbragaglia and S. Succi, Europhys. Lett. **73**, 370 (2006).
[37] X. Shan and X. He, Phys. Rev. Lett. **80**, 65 (1998).
[38] X. He, X. Shan, and G. Doolen, Phys. Rev. E **57**, R13 (1998).
[39] Z. Guo, C. Zheng, and B. Shi, Phys. Rev. E **65**, 046308 (2002).
[40] V. Sofonea and R. F. Sekerka, Phys. Rev. E **71**, 066709 (2005).
[41] S. Chapman and T. G. Cowling, *The Mathematical Theory of Non-uniform Gases* (Cambridge University Press, Cambridge, England, 1970).
[42] C. Cercignani, *The Boltzmann Equation and Its Applications* (Springer-Verlag, New York, 1988).
[43] C. Cercignani, *Slow Rarefied Gas Flows* (Academic Press, City, 2006).
[44] N. G. Hadjiconstantinou, Phys. Fluids **15**, 2352 (2003).
[45] C. Cercignani, *Theory and Application of the Boltzmann Equation* (Academic Press, New York, 1975).
[46] G. A. Bird, *Molecular Dynamics and the Direct Simulation of Gas Flows* (Oxford University Press, Oxford, 1994).
[47] D. A. Lokerby, J. M. Reese, and M. A. Gallis, AIAA J. **43**, 1391 (2005).
[48] Z. Guo, B. Shi, T. S. Zhao, and C. Zheng, Phys. Rev. E **76**, 056704 (2007).
[49] D. A. Lockerby, J. M. Reese, and M. A. Gallis, Phys. Fluids **17**, 100609 (2005).
[50] C. Cercignani, M. Lampis, and S. Lorenzani, Phys. Fluids **16**, 3426 (2004).
[51] D. R. Willis, Phys. Fluids **5**, 127 (1962).
[52] M. Bouzidi, M. Firdaouss, and P. Lallemand, Phys. Fluids **13**, 3452 (2001).